Proc. Natl. Acad. Sci. USA
Vol. 85, pp. 8497–8501, November 1988
Biophysics

Ligand binding to synthetic mutant myoglobin (His-E7 → Gly): Role of the distal histidine

(site-directed mutagenesis)

D. BRAUNSTEIN†, A. ANSARI†, J. BERENDZEN†, B. R. COWEN†, K. D. EGEBERG‡, H. FRAUENFELDER†§, M. K. HONG†, P. ORMOS†¶, T. B. SAUKE†, R. SCHOLL†, A. SCHULTE†, S. G. SLIGAR‡, B. A. SPRINGER‡, P. J. STEINBACH†, AND R. D. YOUNG†‖

†Departments of Physics and Biophysics, and ‡Departments of Biochemistry and Chemistry, University of Illinois at Urbana–Champaign, Urbana, IL 61801

Contributed by H. Frauenfelder, August 8, 1988

ABSTRACT **Low-temperature flash photolysis with IR and visible spectroscopy was used to probe the influence of the distal histidine His-64(E7) of sperm-whale myoglobin (Mb) on the orientation of bound carbon monoxide (CO) and on the kinetics of CO rebinding. The synthesis and high-level expression of a sperm-whale myoglobin gene in *Escherichia coli* permits the efficient substitution of the distal histidine through site-directed mutagenesis. Substitution of His-E7 with glycine [Gly^{E7}]Mb bound with CO (CO[Gly^{E7}]Mb) results in one broad bound-CO IR stretch band, ν(C—O), centered at 1973 cm^{-1} at 10 K, in contrast to three distinct bands for native and synthetic wild-type MbCO at 1966, 1945, and 1929 cm^{-1}. After flash photolysis at 10 K, the unbound state of CO[Gly^{E7}]Mb exhibits two CO stretch bands, whereas MbCO has three. Fourier transform IR spectroscopy measurements of the linear dichroism after photoselective flash photolysis of CO bound to [Gly^{E7}]Mb at 10 K reveals the bound CO to be oriented at an angle of $\alpha = 20° \pm 2°$ with respect to the heme normal. Flash photolysis data from 10 to 300 K provide evidence for a larger distal pocket and a smaller enthalpy barrier (by ≈4 kJ/mol) for [Gly^{E7}]MbCO as compared with wild-type MbCO. These results reinforce the notion that the dominant control of the binding step at the heme iron comes from the proximal side through the protein structure.**

The relation between macromolecular structure and function is one of the most intriguing problems in molecular biology. In the oxygen storage and transport proteins, myoglobin (Mb) and hemoglobin (Hb), a central issue is the role of the protein structure in the selective binding of atmospheric O_2 versus CO to the embedded heme prosthetic group: the binding affinity of CO to protoheme is about 100 times greater than to Mb (1–3). If Mb were to have the same affinity as protoheme, endogenous breakdown of heme would produce enough CO to render oxidative metabolism of O_2 impossible.

Mb and individual Hb chains contain one heme prosthetic group buried in the protein matrix. The heme Fe is coordinated to four pyrrole nitrogens and an imidazole nitrogen donated by the globin proximal histidine [His-93(F8)]. The sixth coordinate position of the iron binds ligands reversibly. Two highly conserved residues in the distal pocket are implicated in the observed ligand-binding selectivity: His-E7 and Val-E11. CO binds to Mb and Hb in a bent or tilted geometry rather than normal to the heme plane (1–6). It is usually assumed that the off-axis position of CO is caused by the steric hindrance of His-E7 and that this hindrance regulates the CO affinity.

Until recently, the effect of various residues on ligand binding was studied by using naturally occurring mutants (7–13). An example is Hb Zürich, in which an arginine replaces His-E7. Such studies imply that His-E7 is important but do not detail its role. Progress in recombinant DNA technology has allowed advances in site-directed mutagenesis. The advantages of specific genetic alteration of key residues are apparent. Nagai and coworkers (14) have successfully used site-directed mutagenesis combined with O_2-binding kinetics, x-ray crystallography, and resonance Raman spectroscopy to probe the function of the His-E7 and Val-E11 residues in Hb β chains.

We combine site-directed mutagenesis with low-temperature Fourier transform IR (FTIR) difference spectroscopy and flash photolysis to probe the role of the His-E7 in Mb. By selecting Mb we avoided the complication of cooperativity. We substituted His-E7 with glycine by taking advantage of the expression of a synthetic sperm-whale Mb gene in *Escherichia coli* (15) and denote the mutated Mb by [Gly^{E7}]Mb. The study of CO rebinding over the temperature range 10–300 K yields insight into the effect of residue substitution on controlling binding at the heme iron. The linear dichroism of FTIR spectra of photoselected samples determines the orientation of the bound CO dipole with respect to the heme normal.

MATERIALS AND METHODS

Sperm-Whale Mb. Mutagenesis of the synthetic Mb gene was performed by inserting oligonucleotides coded for glycine in place of histidine at position E7 (S.G.S., unpublished data). The synthetic form has an additional methionine at the amino terminus not present in the native Mb (Sigma), but optical and magnetic spectroscopy show no significant differences between the synthetic wild-type and native Mbs (15).

FTIR Spectroscopy. The CO stretch bands, ν(C—O), in the bound (A) and the photodissociated (B) states were measured on a Mattson Sirius 100 FTIR spectrometer. Lyophilyzed protein was dissolved in a 75% glycerol/water (vol/vol) solvent buffered to ≈pH 7 with 0.1 M potassium phosphate and an excess of sodium dithionite. The final protein concentration ([Gly^{E7}]Mb) was 3 mM. Approximately 10 μl of solution was placed between two CaF_2 windows separated by a 75-μm spacer. A closed-cycle helium refrigerator (CTI Cryogenics, model 21) cooled the sample. All spectra were taken at 2 cm^{-1} resolution and at 10 K, where rebinding of the

The publication costs of this article were defrayed in part by page charge payment. This article must therefore be hereby marked "*advertisement*" in accordance with 18 U.S.C. §1734 solely to indicate this fact.

Abbreviations: FTIR, Fourier transform infrared; Mb, myoglobin; [Gly^{E7}]Mb, His-64(E7) → Gly substitution in wild-type Mb.

§To whom reprint requests should be addressed at: Department of Physics, University of Illinois, 1110 West Green Street, Urbana, IL 61801.

¶Permanent address: Institute of Biophysics, Hungarian Academy of Sciences, Odesszai Krt. 62, 6701 Szeged, Hungary.

‖Permanent address: Department of Physics, Illinois State University, Normal, IL 61761.

ligand is slow on the time scale of the measurement. The absorption difference spectra were obtained by referencing the photolyzed spectrum to the unphotolyzed background (Mb*/MbCO). Photolysis was achieved with a tungsten lamp (Oriel, 250 W).

Photoselection and Linear Dichroism. The angle of the CO dipole with respect to the heme normal can be determined by measuring the linear dichroism of a partially photolyzed sample in the IR at low temperature (16). In photoselection, linearly polarized light filtered to 540 ± 5 nm partially photolyzes the sample. This wavelength corresponds to the heme β band, for which the transition dipole is isotropic in the heme plane (17). We then determine the orientation of the CO dipole relative to the transition dipole of the β band by measuring the IR spectra with the polarization parallel and perpendicular to the polarization of the photolyzing beam. An IR polarizer (model IGP228, Molectron, Sunnyvale, CA) produced the two polarizations. The angle α between the heme normal and the ν(C—O) transition dipole is given by $\alpha = \sin^{-1}\{[4(I_{\parallel}/I_{\perp}) - 2]/[(I_{\parallel}/I_{\perp}) + 2]\}^{1/2}$ where $I_{\parallel}$ and $I_{\perp}$ are the parallel and perpendicular intensities, respectively (16). Because the IR transition dipole lies along the C—O bond axis, α gives the angle between the CO axis and the heme normal.

Flash Photolysis. The flash photolysis system employed a 30-nsec pulse from a frequency-doubled, Q-switched Nd^+-glass laser (540 nm, 240 mJ). Samples consisted of protein dissolved in a 75% glycerol/water solvent buffered to pH 7.0 with 20 mM potassium phosphate and an excess of sodium dithionite. The final protein concentration ([Gly^{E7}]Mb) was ≈20 μM. Rebinding was monitored with light from a tungsten lamp passed through a monochromator at 440 nm and measured by a photomultiplier (Hamamatsu 928). The signal was digitized from 1 μsec to 300 sec by a homebuilt microprocessor-based digitizer with a logarithmic time base. A liquid-helium storage dewar (Janis) permitted temperature control.

RESULTS AND DISCUSSION

Synthetic MbCO. The FTIR absorption difference spectra of synthetic wild-type and native MbCO at 10 K (Fig. 1) show the ν(C—O) bands of the bound (A) and the photolyzed (B) states (18, 19). No significant differences between the native and synthetic wild-type MbCO were observed in the peak positions of the photodissociated and bound CO stretch bands, the angle of the bound ligand as determined by linear dichroism following photoselection, or the CO-rebinding kinetics. Differences in the peak intensities of the bands between the two spectra can be attributed to slightly different pH values. Therefore, any new phenomena seen in the mutant Mb are caused by the exchange of the His-E7 for glycine and are not artifacts of the synthesis of Mb in *E. coli*.

Static Properties. A striking difference between MbCO and CO[Gly^{E7}]Mb is seen in the 10 K FTIR absorption difference spectra in Figs. 1 and 2. MbCO shows three distinct bands, which we interpret following Makinen *et al.* (19, 20), as three distinct conformational substates corresponding to three different protein structures. In contrast, CO[Gly^{E7}]Mb possesses only one broad band centered at 1973 cm^{-1}. Preliminary rebinding kinetics following flash photolysis at 50 K indicates that the band is composed of two components. The small peak at 1930 cm^{-1} is the red-shifted stretch band caused by the small fraction of ^{13}C in the CO. The three substates in MbCO have angles α as given in Table 1, whereas CO[Gly^{E7}]Mb has an angle $\alpha = 20°$. The absence of His-E7 thus results in a CO orientation similar to that of substate A_0 in wild-type MbCO. The photolyzed state, Mb*, exhibits three B substates (Fig. 1*b*), whereas [Gly^{E7}]Mb* shows only two broad bands (Fig. 2). Neither the B substates of Mb* nor of [Gly^{E7}]Mb* show a linear dichroism (16). We summarize

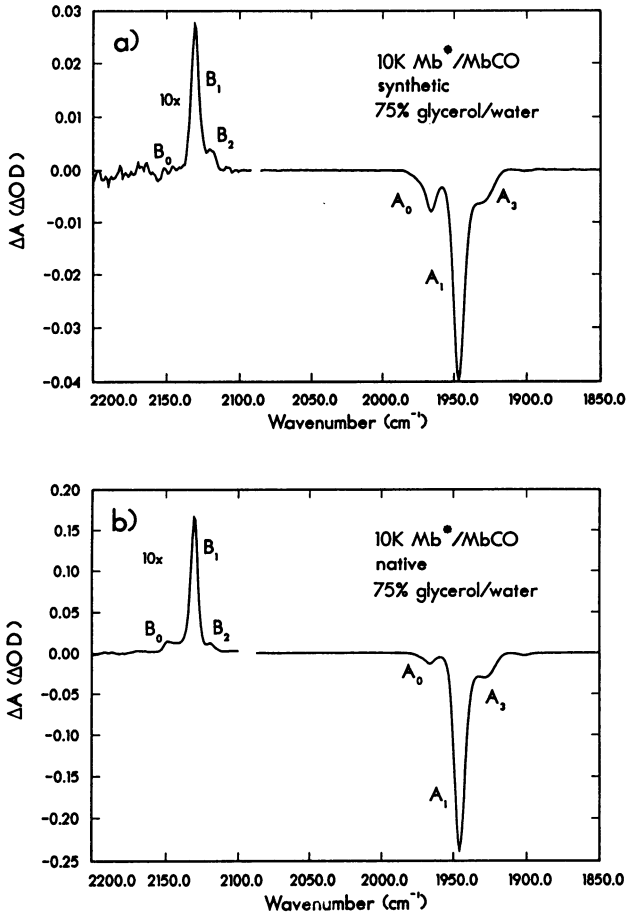

FIG. 1. FTIR absorption difference spectrum of synthetic wild-type Mb*/MbCO (*a*) and native Mb*/MbCO (*b*) at 10 K in 75% glycerol/water at ≈pH 7.

in Table 1 the static properties of the native and mutant MbCO. The changes in the conformations for [Gly^{E7}]Mb in the bound and photolyzed states are evidence for the crucial role played by the distal histidine in determining the ligand–heme conformation.

Low-Temperature CO Rebinding. The rebinding of CO to [Gly^{E7}]Mb also sheds light on the role of the distal histidine. We measured rebinding kinetics of CO[Gly^{E7}]Mb after flash photolysis from 10 to 300 K at 440 nm in 75% glycerol/water (Figs. 3 and 5). The low-temperature data show smooth nonexponential kinetics as seen in all heme protein systems

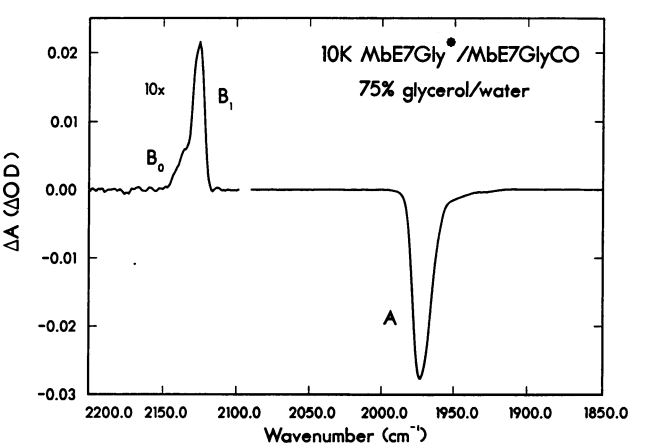

FIG. 2. FTIR absorption difference spectrum of [Gly^{E7}]-Mb*/CO[Gly^{E7}]Mb (MbE7Gly*/MbE7GlyCO) at 10 K in 75% glycerol/water at ≈pH 7.

Table 1. Parameters of the A and B substates in MbCO and CO[Gly^{E7}]Mb

	Substate	ν, cm^{-1}	Γ(FWHM), cm^{-1}	α
MbCO*	A_0	1966	9.7	15° ± 3°
	A_1	1945	8.8	28° ± 2°
	A_3	1929	14.0	33° ± 4°
	B_0	2149	6.0	—
	B_1	2130	6.3	—
	B_2	2119	7.0	—
CO[Gly^{E7}]Mb†	A	1973	14.9	20° ± 2°
	B_0	2137	13.6	—
	B_1	2125	7.6	—

All data refer to 75% glycerol/water solvent at 10 K and pH 7. Γ(FWHM), full width at half-maximum.
*Refs. 16 and 19.
†Data from present work.

studied (21, 22). We fit the data from 60 to 160 K by assuming a distribution of conformational substates with different barriers for rebinding (21). Below ≈180 K in a 75% glycerol/water solvent the ligand is confined to the heme pocket, and each protein molecule is frozen in a conformational substate with a specific activation enthalpy for rebinding. We define $g(H)dH$ as the probability of a protein having an activation enthalpy between H and $H + dH$. The fraction of proteins that have not yet rebound a ligand at time t then becomes

$$N(t, T) = \int_0^\infty g(H)e^{-k_{BA}(H,T)t}dH. \quad [1]$$

The rate coefficient is given by

$$k_{BA}(H, T) = A_{BA}(T/T_o)e^{-H/RT}, \quad [2]$$

$$A_{BA} = \nu e^{S/R}, \quad [3]$$

where S is the activation entropy, R = 8.314 J/mol-K, T_o is taken to be 100 K, and ν is the attempt frequency at 100 K. $N(t, T) = \Delta A(t, T)/\Delta A(0, T)$, where $\Delta A(0, T)$ was assumed to be 2.34 OD at all temperatures. We parameterize $g(H)$ as a gamma distribution (23) and show the distributions obtained for mutant and native MbCO in Fig. 4. The solid lines in Fig. 3 are a least-squares fit using a finite-difference Levenberg–Marquardt algorithm to minimize χ^2. The peak enthalpies and preexponentials are listed in Table 2. The reduction in the peak enthalpy reflects the reduced hindrance experienced by the ligand in rebinding to the glycine mutant; the reduction in the preexponential can be attributed to the increased entropy of the mutant–ligand system in state B owing to the larger distal pocket in the glycine mutant (24).

In native Mb the distal histidine affects binding both sterically and electrostatically (6, 25–30). Comparing the CO

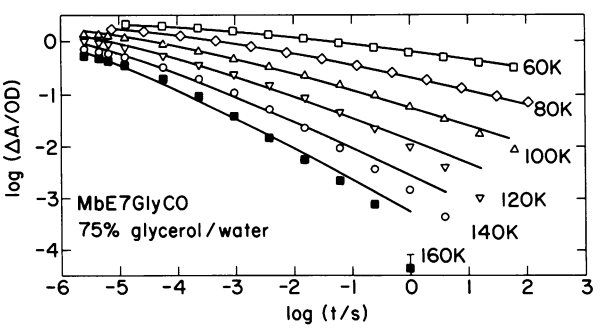

FIG. 3. Recombination of CO with [Gly^{E7}]Mb (MbE7GlyCO) over the temperature range 60–160 K in 75% glycerol/water, pH 7. The solid lines are fits based on Eqs. (1 and 2) and the enthalpy distribution given in Fig. 4.

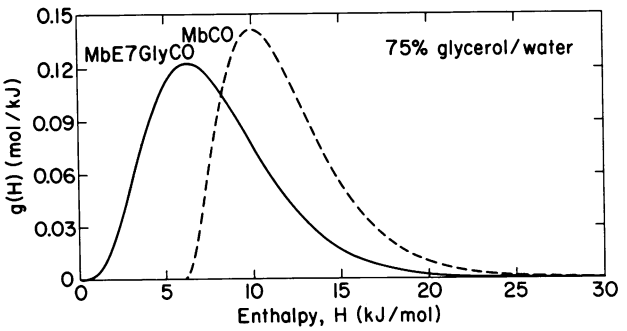

FIG. 4. Activation enthalpy spectra of the innermost barrier B → A of CO[Gly^{E7}]Mb (MbE7GlyCO) and MbCO. $g(H)dH$ denotes the probability of a protein having an activation enthalpy between H and $H + dH$.

rebinding of wild-type Mb with that of separated β chains of hemoglobin Zürich, in which the His-E7 is replaced by an arginine (30), suggests that the steric effect of His-E7 accounts for 2 kJ/mol of the enthalpy barrier. The electrostatic effect has been estimated from the pH dependence of the CO rebinding to Mb. The pH dependence has been interpreted in terms of a charge–dipole interaction between the CO dipole and the positive charge of the imidazole of the His-E7 (30). The faster rebinding at pH 5 suggests that the charge of the distal histidine can contribute 2–4 kJ/mol to the enthalpy barrier. The reduction in the peak enthalpy of 4 kJ/mol in the glycine mutant is consistent with these previous estimates.

The rebinding kinetics also differentiates the role of entropy and enthalpy in the bond formation step, B → A, at the heme iron. The single CO conformation in CO[Gly^{E7}]Mb appears to be related to the A_0 substate in MbCO because the orientation angle α and peak frequencies are comparable (Table 1). Average binding rates of the two states at 100 K are also similar (Table 2). However, the binding rates are larger than that measured in MbCO at 440 nm for different reasons: the A_0 substate in MbCO binds faster because of its larger preexponential—i.e., an entropy effect—whereas the A state in CO[Gly^{E7}]Mb binds faster because of a smaller enthalpy barrier. Thus, the distal histidine influences both the entropy and enthalpy barriers for CO rebinding to the heme iron.

High-Temperature Binding. Fig. 5 shows that rebinding becomes more complicated above ≈200 K. The slowest process, denoted by S, is proportional to the ligand concentration in the solvent. We interpret S as the solvent process: CO escapes from the pocket into the solvent and rebinds from there (30, 31). In Mb and in [Gly^{E7}]Mb process S is exponential. In [Gly^{E7}]Mb, an additional slow component with an amplitude of a few percent occurs, the origin of which is unclear. The association rate coefficient λ_{on} for process S can be written as (30–32)

$$\lambda_{on}(T) = \bar{k}_{BA}(T)P_B(T)N_s(T). \quad [4]$$

Table 2. Parameters for CO binding to Mb and [Gly^{E7}]Mb in 75% glycerol/water, pH 7, at 1 atm CO

Parameter	CO[Gly^{E7}]Mb,* 440 nm	MbCO,* 440 nm	MbCO,† A_0
H_{peak}(kJ/mol)	6.3 ± 0.2	10.0 ± 0.2	10
log[A_{BA}/sec^{-1}]	8.4 ± 0.1	9.0 ± 0.1	10.8
log[$\bar{k}_{BA}$/sec^{-1}] (100 K)	6.1	4.3	6.3
log[$\bar{k}_{BA}$/sec^{-1}] (300 K)	7.4	7.4	—
log[λ_{on}/sec^{-1}] (300 K)	3.7	2.8	—
N_s (300 K)	0.47 ± 0.02	≈1	—
log P_B (300 K)	−3.4	−4.6	—

*Data from present work.
†Ref. 19.

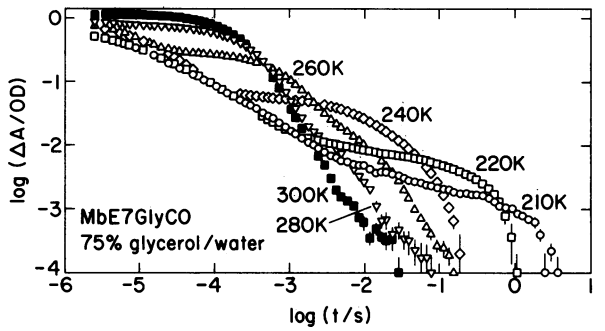

FIG. 5. Recombination of CO with [Gly^{E7}]Mb (MbE7GlyCO) over the temperature range 210–300 K in 75% glycerol/water, pH 7, at 1 atm of CO (1 atm = 101.3 kPa).

Here $\bar{k}_{BA}(T)$ is the average rate coefficient for the step B → A extrapolated to the temperature T (23). $P_B(T)$ is an occupation factor, which in the limit $k_{BA} \rightarrow 0$, is the probability of finding the system in state B. N_s is the fraction of ligands that reach the solvent after being photodissociated. Values of N_s (assuming a temperature-independent change in absorbance), λ_{on}, the extrapolated $\bar{k}_{BA}$, and the resultant P_B at 300 K are given in Table 2. The data are surprising: the average rates $\bar{k}_{BA}$ for the binding step at the heme iron, extrapolated from the low-temperature data to 300 K, are nearly the same for Mb and [Gly^{E7}]Mb. The difference in the association rate coefficient λ_{on} between Mb and [Gly^{E7}]Mb is predominantly caused by the larger P_B for the mutant.

The extrapolation used here assumes that protein relaxation above 200 K does not shift the distributions $g(H)$ shown in Fig. 4. If such a shift occurs, as predicted by Agmon and Hopfield (33), the extrapolated values of k_{BA} and $P_B(T)$ will change, but we expect the main conclusions to remain valid.

Pocket Volumes. The volumes of the pocket in Mb and [Gly^{E7}]Mb can be estimated in a number of ways. First, we note that the two amino acids have very different volumes, V_{His}, ≈153 Å^3 and V_{Gly}, ≈60 Å^3 (34). If the overall protein structure does not change drastically, we expect the pocket in the mutant to be larger by ≈90 Å^3. The larger pocket volume should be observable as a larger entropy change in binding, and hence [Gly^{E7}]Mb should have a smaller preexponential, A_{BA}, than native Mb. Table 2 confirms this expectation. The larger pocket volume should also appear as a larger factor P_B, and this prediction is also correct. While all our data are consistent with a much larger volume in [Gly^{E7}]Mb than in Mb, it is difficult to give a definite value for the pocket volume ratio, because Mb exists in three A substates, whereas [Gly^{E7}]Mb assumes only one conformation.

The larger pocket should have another effect: A reduced preexponential for the step B → A implies a larger preexponential for the dissociation step A → B (24). Even if the replacement His-E7 → Gly does not change the binding enthalpy of the CO, the larger pocket volume should increase A_{AB} and hence $\bar{k}_{AB}$. Indeed, the CO-off rate increases by about a factor of 2 (S.G.S., unpublished data). Because the fraction N_s (Eq. 4) given in Table 2 is ≈0.5, $\bar{k}_{AB}$ must increase by about a factor 4.

CONCLUSION

In the present work we studied the effect of replacing the distal histidine in myoglobin, His-E7, with glycine. The result differs from what we anticipated. Textbooks assert that His-E7 forces the bound CO into a bent position, away from the heme normal, thereby decreasing the association rate and lowering the affinity (1). We therefore expected the replacement His-E7 → Gly to result in a heme-normal–CO angle of 0° and a much larger rate coefficient k_{BA}. The experiments show, however, that the association and dissociation rates increase only moderately, so that the equilibrium rate coefficient (k_{BA}) is larger by only a factor of five (S.G.S., unpublished data). The coefficient $\bar{k}_{BA}$ at 300 K is little changed and is not nearly as large as for protoheme (35), reinforcing the notion that the dominant control of the binding step at the heme iron comes from the proximal side (30, 36, 39). Moreover, the angle between the CO and the heme normal is still ≈20°. Because the CO in the absence of steric effects is expected to lie in the heme normal (37), steric effects may still be present, caused for instance by Val-E11. The replacement of histidine by glycine also affects dioxygen. [Gly^{E7}]Mb was found to autooxidize much more rapidly than wild-type protein (S.G.S., unpublished data), thus making low-temperature ligand-binding experiments more difficult.

The multiple A substates shown in Fig. 1 invite the question as to their role. Multiple bound substates have also been seen in elephant MbCO, where the His-E7 is replaced with a glutamine (38). IR measurements on mutants in which the distal histidine is replaced by amino acids with nonpolar side chains, however, show only one A substate. His-E7 and Gln-E7 thus also play a crucial role in promoting the multiplicity of CO orientations in MbCO. The role of the multiple A substates in the function of Mb is not yet understood, and it is therefore not clear whether the multiple A substates caused by His-E7 or Gln-E7 are a side effect or are truly important.

We thank Stan Luck and Tim Iben for technical assistance and helpful discussions. We thank John Kuriyan and Dagmar Ringe for providing the x-ray coordinates of MbCO. Discussions with Anders Ehrenberg and K. G. Paul clarified many points. R.D.Y. acknowledges research support from Illinois State University. This work was supported in part by National Institutes of Health Grants GM 18051, GM 32455, GM 33775, and GM 31756, and National Science Foundation Grant DMB88-16476.

1. Stryer, L. (1988) *Biochemistry* (Freeman, New York), pp. 148–150.
2. Collman, J. P., Brauman, J. I., Halpert, T. R. & Suslick, K. S. (1976) *Proc. Natl. Acad. Sci. USA* **73**, 3333–3337.
3. Dickerson, R. E. & Geis, I. (1983) *Hemoglobin, Structure, Function, Evolution and Pathology* (Benjamin Cummings, Menlo Park, CA), p. 30.
4. Norvell, J. C., Nunces, A. C. & Schoenborn, B. P. (1975) *Science* **190**, 568–569.
5. Baldwin, J. M. (1980) *J. Mol. Biol.* **136**, 103–128.
6. Satterlee, J. D., Teintze, M. & Richards, J. (1978) *Biochemistry* **17**, 1456–1462.
7. Antonini, E. & Brunori, M. (1971) *Hemoglobin and Myoglobin in Their Reactions with Ligands* (American Elsevier, New York).
8. Giacometti, G. M., DiIorio, E. E., Antonini, E., Brunori, M. & Winterhalter, K. H. (1977) *Eur. J. Biochem.* **75**, 267–273.
9. Imai, K., Ikeda-Saito, M. & Yonetani, T. (1980) *J. Mol. Biol.* **144**, 551–565.
10. Heidner, E. J., Ladner, R. C. & Perutz, M. F. (1976) *J. Mol. Biol.* **104**, 707–722.
11. Ikeda-Saito, M., Iizuka, T., Yamamoto, H., Kayne, I. J. & Yonetani, T. (1977) *J. Biol. Chem.* **252**, 4882–4887.
12. Caughey, W. S., Alben, J. O., McCoy, S., Boyer, S., Charache, S. & Hathaway, P. (1969) *Biochemistry* **8**, 59–62.
13. Dlott, D. D., Frauenfelder, H., Langer, P., Roder, H. & DiIorio, E. E. (1983) *Proc. Natl. Acad. Sci. USA* **80**, 6239–6243.
14. Nagai, K., Luisi, B., Shih, D., Miyazaki, G., Imai, K., Poyart, C., DeYoung, A., Kwiatkowski, L., Noble, R. W., Lin, S.-H. & Yu, N.-T. (1987) *Nature (London)* **329**, 858–860.
15. Springer, B. A. & Sligar, S. G. (1987) *Proc. Natl. Acad. Sci. USA* **84**, 8961–8965.
16. Ormos, P., Braunstein, D., Frauenfelder, H., Hong, M. H., Lin, S.-L., Sauke, T. B. & Young, R. D. (1988) *Proc. Natl. Acad. Sci. USA* **85**, 8492–8496.

17. Eaton, W. A., Hanson, L. K., Stephens, P., Sutherland, J. C. & Dunn, B. R. (1978) *J. Am. Chem. Soc.* **100,** 4991–5003.
18. Alben, J. O., Beece, D., Bowne, S. F., Doster, W., Eisenstein, L., Frauenfelder, H., Good, D., McDonald, J. D., Marden, M. L., Moh, P. P., Reinisch, L., Reynolds, A. H., Shyamsunder, E. & Yue, K. T. (1982) *Proc. Natl. Acad. Sci. USA* **79,** 3744–3748.
19. Ansari, A., Berendzen, J., Braunstein, D., Cowen, B. R., Frauenfelder, H., Hong, M. K., Iben, I. E. T., Johnson, J. B., Ormos, P., Sauke, T. B., Scholl, R., Schulte, A., Steinbach, P. J., Vittitow, J. & Young, R. D. (1987) *Biophys. Chem.* **26,** 337–355.
20. Makinen, M. W., Houtchens, R. A. & Caughey, W. S. (1979) *Proc. Natl. Acad. Sci. USA* **76,** 6042–6046.
21. Austin, R. H., Beeson, K. W., Eisenstein, L., Frauenfelder, H. & Gunsalus, I. C. (1975) *Biochemistry* **14,** 5355–5373.
22. Frauenfelder, H., Parak, F. & Young, R. D. (1988) *Annu. Rev. Biophys. Biophys. Chem.* **17,** 451–479.
23. Young, R. D. & Bowne, S. F. (1984) *J. Chem. Phys.* **81,** 3730–3737.
24. Frauenfelder, H. & Wolynes, P. G. (1985) *Science* **229,** 337–345.
25. Collman, J. P., Brauman, J. & Doxsee, K. (1979) *Proc. Natl. Acad. Sci. USA* **76,** 6035–6039.
26. Stryer, C., Kendrew, J. C. & Watson, H. C. (1964) *J. Mol. Biol.* **8,** 96–104.
27. Caughey, W. S. (1970) *Ann. N.Y. Acad. Sci.* **174,** 148–153.
28. Barlow, C. H., Ohlsson, P. I. & Paul, K. G. (1976) *Biochemistry* **15,** 2225–2229.
29. Kuriyan, J., Wiltz, S., Karplus, M. & Petsko, G. A. (1986) *J. Mol. Biol.* **192,** 133–154.
30. Doster, W., Beece, D., Bowne, S. F., DiIorio, E. E., Eisenstein, L., Frauenfelder, H., Reinisch, L., Shyamsunder, E., Winterhalter, K. H. & Yue, K. T. (1982) *Biochemistry* **21,** 4831–4839.
31. Ansari, A., DiIorio, E. E., Dlott, D. D., Frauenfelder, H., Iben, I. E. T., Langer, P., Roder, H., Sauke, T. B. & Shyamsunder, E. (1986) *Biochemistry* **25,** 3139–3146.
32. Young, R. D. (1984) *J. Chem. Phys.* **80,** 554–560.
33. Agmon, N. & Hopfield, J. J. (1983) *J. Chem. Phys.* **79,** 2042–2053.
34. Zamyatnin, A. A. (1972) *Prog. Biophy.* **24,** 107–123.
35. Alberding, N., Austin, R. H., Chan, S. S., Eisenstein, L., Frauenfelder, H., Gunsalus, I. C. & Nordlund, T. M. (1976) *J. Chem. Phys.* **65,** 4701–4711.
36. Campbell, B. F., Chance, M. R. & Friedman, J. M. (1987) *J. Biol. Chem.* **262,** 14885–14890.
37. Li, X. Y. & Spiro, T. G. (1988) *J. Am. Chem. Soc.* **110,** 6024–6033.
38. Kerr, E. A., Yu, N.-T., Bartnicki, D. E. & Mizukami, H. (1985) *J. Biol. Chem.* **260,** 8360–8365.
39. Giacometti, G. M., Traylor, T. G., Ascenzi, P., Brumori, M. & Antonini, E. (1977) *J. Biol. Chem.* **252,** 7447–7448.